

Research Paper

Structure-based design and in-parallel synthesis of inhibitors of AmpC β -lactamase

Donatella Tondi ^{a,b,1}, Rachel A. Powers ^{a,1}, Emilia Caselli ^{a,b}, María-Cristina Negri ^c, Jesús Blázquez ^c, Maria Paola Costi ^{b,2}, Brian K. Shoichet ^{a,*}

^aDepartment of Molecular Pharmacology and Biological Chemistry, Northwestern University, 303 East Chicago Avenue, Chicago, IL 60611, USA

^bDipartimento di Scienze Farmaceutiche, Università degli Studi di Modena e Reggio Emilia, Via Campi 183, Modena, Italy

^cServicio de Microbiología, Hospital Ramón y Cajal, Ctra. Colmenar Km 9.100, 28034 Madrid, Spain

Received 8 January 2001; accepted 23 March 2001

First published online 8 May 2001

Abstract

Background: Group I β -lactamases are a major cause of antibiotic resistance to β -lactams such as penicillins and cephalosporins. These enzymes are only modestly affected by classic β -lactam-based inhibitors, such as clavulanic acid. Conversely, small arylboronic acids inhibit these enzymes at sub-micromolar concentrations. Structural studies suggest these inhibitors bind to a well-defined cleft in the group I β -lactamase AmpC; this cleft binds the ubiquitous R1 side chain of β -lactams. Intriguingly, much of this cleft is left unoccupied by the small arylboronic acids.

Results: To investigate if larger boronic acids might take advantage of this cleft, structure-guided in-parallel synthesis was used to explore new inhibitors of AmpC. Twenty-eight derivatives of the lead compound, 3-aminophenylboronic acid, led to an inhibitor with 80-fold better binding (**2**; K_i 83 nM). Molecular docking suggested orientations for this compound in the R1 cleft. Based on the docking results, 12 derivatives of **2** were synthesized, leading to inhibitors with K_i values of 60 nM and with improved solubility. Several of these inhibitors reversed the resistance of nosocomial Gram-positive bacteria, though they showed little activity against Gram-negative bacteria. The X-ray crystal

structure of compound **2** in complex with AmpC was subsequently determined to 2.1 Å resolution. The placement of the proximal two-thirds of the inhibitor in the experimental structure corresponds with the docked structure, but a bond rotation leads to a distinctly different placement of the distal part of the inhibitor. In the experimental structure, the inhibitor interacts with conserved residues in the R1 cleft whose role in recognition has not been previously explored.

Conclusions: Combining structure-based design with in-parallel synthesis allowed for the rapid exploration of inhibitor functionality in the R1 cleft of AmpC. The resulting inhibitors differ considerably from β -lactams but nevertheless inhibit the enzyme well. The crystal structure of **2** (K_i 83 nM) in complex with AmpC may guide exploration of a highly conserved, largely unexplored cleft, providing a template for further design against AmpC β -lactamase. © 2001 Elsevier Science Ltd. All rights reserved.

Keywords: Antibiotic resistance; Structure-based drug design; Boronic acids; Transition-state analog; X-ray crystallography

1. Introduction

β -Lactamases catalyze the hydrolysis of β -lactam anti-

biotics, deactivating them. These enzymes are the most widespread resistance mechanism to drugs of the penicillin and cephalosporin families, and they threaten public health [1,2]. To combat these enzymes, medicinal chemists have introduced β -lactam-based inhibitors, such as clavulanic acid, and ' β -lactamase-resistant' β -lactams, such as aztreonam [3,4]. These anti-resistance β -lactams resemble the original penicillins and cephalosporins; like the early penicillins and cephalosporins, many of them are natural products or simple derivatives of natural products. The exposure of bacteria to these compounds over evolutionary time [5] has allowed bacteria to rapidly acquire resistance to these anti-resistance drugs [6]. To escape from this

Abbreviations: DVB, divinyl-benzene; TLC, thin layer chromatography; MIC, minimum inhibitory concentration; SAR, structure-activity relationship

¹ These authors contributed equally to this paper.

² Also corresponding author: E-mail: costimp@mail.unimo.it

* Correspondence: Brian K. Shoichet;
E-mail: b-shoichet@northwestern.edu

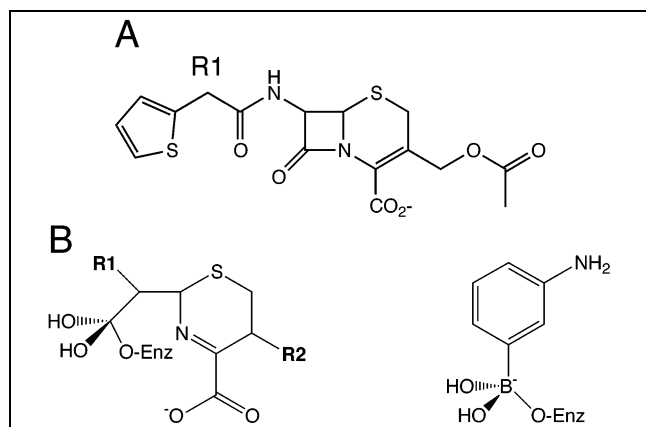


Fig. 1. (A) A characteristic cephalosporin, cephalothin. The R1 side chain is labeled. (B) Comparison between the deacylation high energy intermediate of a cephalosporin in a serine β -lactamase and the transition-state analog formed by a boronic acid and the same enzyme. The protonation state of the high-energy intermediate remains an area of research [13,15].

cycle of small modification and rapid response, it is worthwhile to explore non- β -lactam inhibitors of β -lactamases.

An interesting class of non- β -lactam inhibitors of serine β -lactamases is the boronic acids [7–12]. These molecules act competitively, forming reversible adducts with the cat-

alytic serine of the enzymes, adopting a tetrahedral geometry thought to resemble that of the high energy intermediate (Fig. 1). Although the original leads had only modest affinity for β -lactamases [7], structure-based design has recently led to inhibitors with nanomolar affinities [8,9,11] and anti-microbial activity at low $\mu\text{g/ml}$ concentrations [9,10,12]. The arylboronic acids vary in affinity for the group I β -lactamase AmpC by four orders of magnitude. This is consistent with modeling [9] and crystallographic studies [10,13] that suggest that affinity for the enzyme is modulated by the aryl side chains of the inhibitors. These interactions take place in the part of the AmpC cleft thought to be responsible for binding the R1 side chains of β -lactams [12,14–16] (Fig. 1); we will refer to this region as the ‘R1 cleft’ of the enzyme (Fig. 2).

Most of the arylboronic acids investigated to date have been small. Although highly complementary to the enzyme in the region where they bind, much of the cleft is left open by these inhibitors [10] (Fig. 2). We wondered whether larger inhibitors might take advantage of this open region, and if so, what sort of functionality would best complement it. The surface of the R1 cleft contains a number of indentations, and the surface-exposed residues that line it are highly conserved (Fig. 2), suggesting that several binding sites may be available. Conversely, the

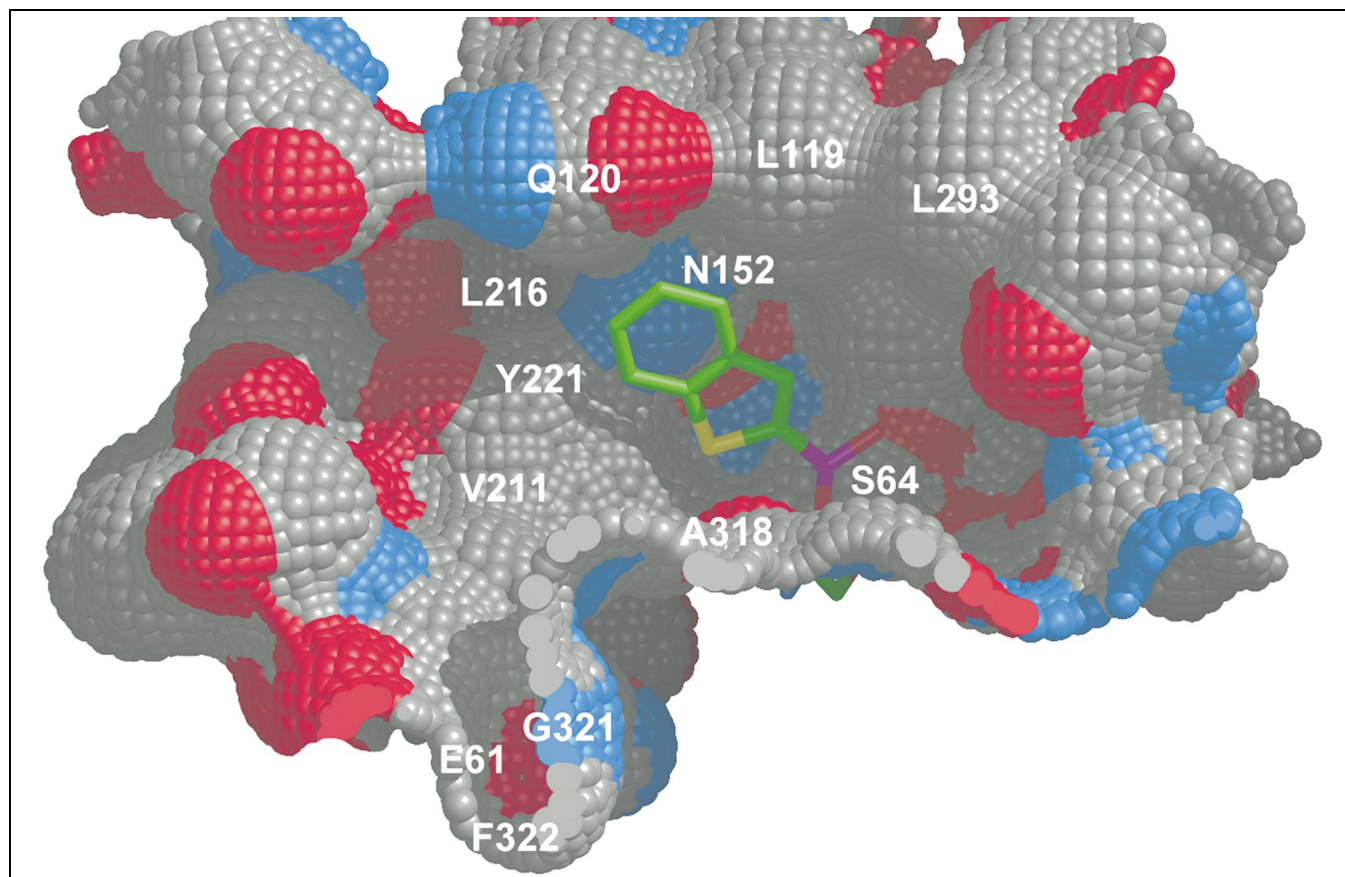


Fig. 2. The molecular surface of the R1 cleft of AmpC β -lactamase from *Escherichia coli* in complex with benzo(b)thiophene-2-boronic acid [10]. Some conserved amino acids in this cleft are labeled. Figs. 2, 4, 6, and 7 were generated with MidasPlus [50].

Table 1
Inhibitors of AmpC synthesized through in-parallel techniques

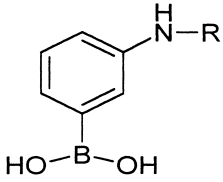
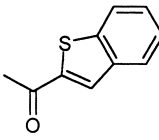
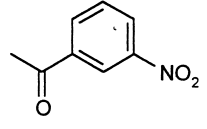
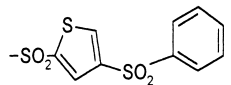
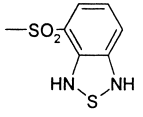
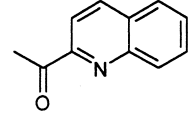
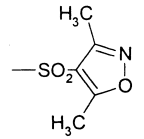
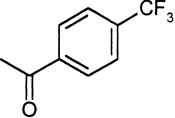
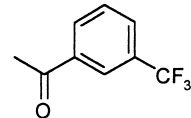
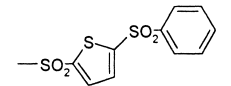
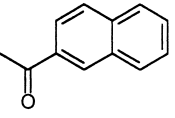
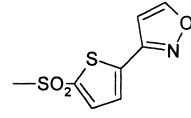
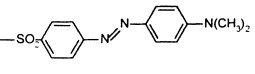
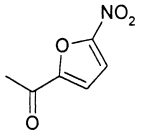
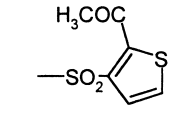
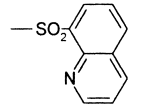
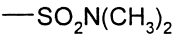
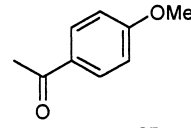
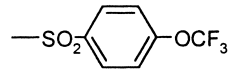
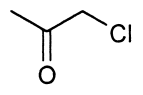
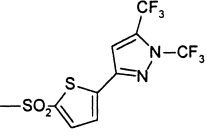
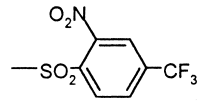
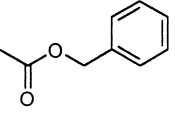
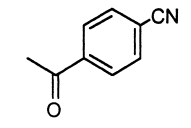
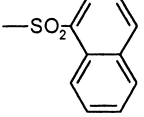
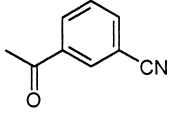
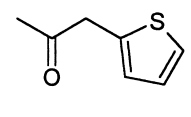
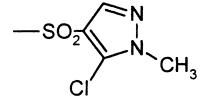
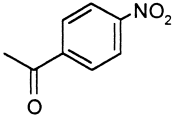
								
code	structure (R)	K_i (μM)	code	structure (R)	K_i (μM)	code	structure (R)	K_i (μM)
1	H	7.3	11		1.6	21		8.3
2		0.08	12		1.6	22		12.3
3		0.10	13		2.5	23		12.0
4		0.12	14		4.0	24		12.3
5		0.53	15		4.0	25		13.2
6		0.66	16		5.5	26		14.1
7		0.70	17		7.2	27		15.5
8		0.82	18		8.2	28		16.5
9		1.30	19		8.2	29		25.0
10		1.6	20		8.3			

Table 2
 Focused library based on compound 2

code	structure (R)	K_i (μM)	code	structure (R)	K_i (μM)
30		0.68	36		0.62
31		0.86	37		0.90
32		1.02	38		0.77
33		0.06	39		1.2
34		0.20	41		0.08
35		0.45	42		0.34

function of most of this region is unknown, and there is little structure–activity information to guide inhibitor design.

Taking advantage of open clefts is a common problem in structure-based inhibitor design. The possibility of designing functionality for these sites is one of the advantages of working with atomic resolution structures. Because they are new sites, designing appropriate ligand functionality to complement them is challenging. This is a question not only of predicting favorable interactions,

which is difficult in an aqueous environment [17], but also of coordinating the design with synthetic feasibility.

To address this question, we adopted a strategy of structure-guided in-parallel synthesis. This technique can rapidly explore derivatives of a lead compound [18,19]. The ligand functionality explored can be constrained by receptor structural information [20,21], and the structures of interesting compounds in complex with the enzyme provide templates for further design. A known inhibitor, 3-aminophenylboronic acid [7,13] (1, Table 1), was used

as the lead for the in-parallel syntheses. Although **1** is only a modest inhibitor of AmpC (K_i 7.3 μ M) [7], it is well suited to derivatization. Modeling studies suggested that amide and sulfonamide derivatives of **1** would fit well into the R1 cleft of AmpC [9]. Twenty-eight derivatives were synthesized through polymer-assisted in-parallel chemistry, resulting in several inhibitors that bound in the 100 nM range. Flexible ligand docking calculations [22] suggested a conformation of one of these inhibitors, compound **2**, in the R1 cleft of AmpC. Based on this prediction, a second, focused library of 12 molecules was synthesized to improve solubility and inhibition and to explore the structure–activity relationships (SAR) of the series (Table 2). Subsequently, the structure of **2** bound to AmpC was determined by X-ray crystallography to 2.1 Å resolution. This structure allows us to probe new recognition elements in the R1 cleft and to determine how well our docking model predicted the experimental binding geometry. The structure provides a template for further design in this series of β -lactamase inhibitors.

2. Library design

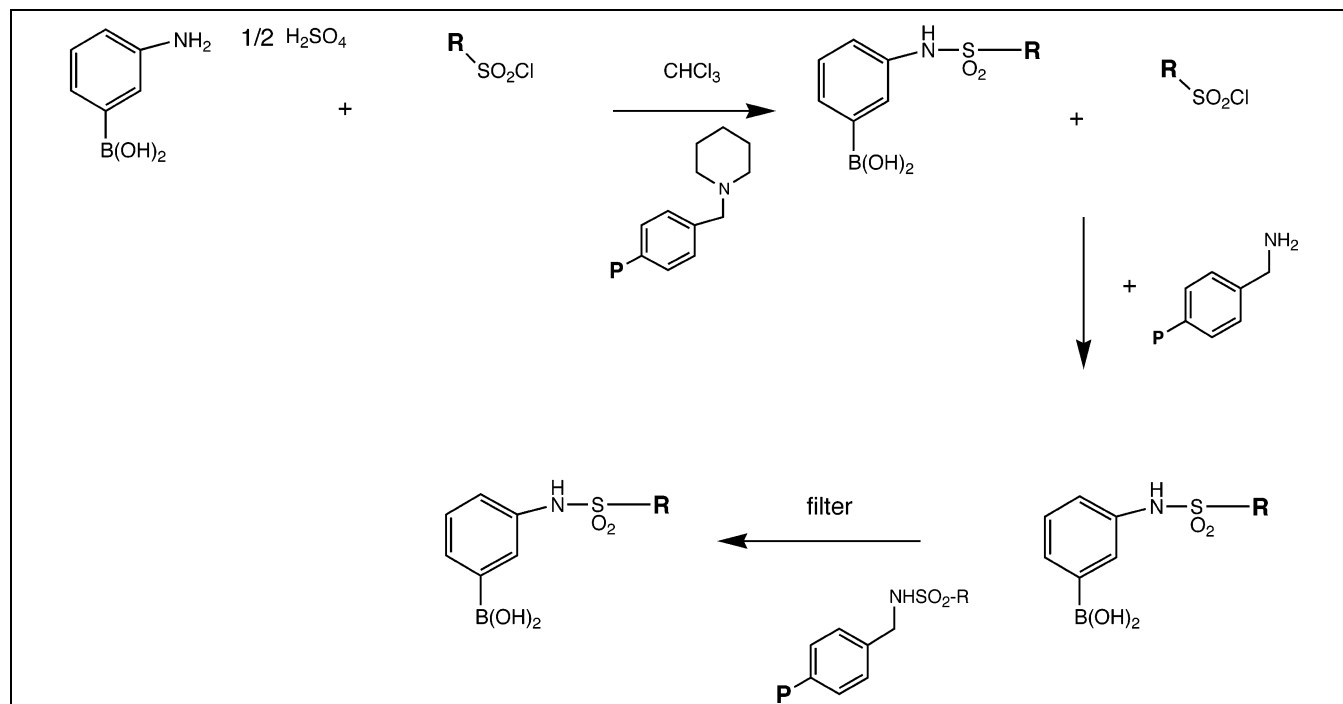
Previous studies of boronic acid adducts of AmpC suggested that amide and sulfonamide derivatives could be accommodated in the AmpC site [9]. The library was designed to explore a relatively diverse group of such derivatives, taking advantage of the well-understood chemistry afforded by amide and sulfonamide linkers. A substructure search of the Available Chemicals Database using the ISIS program (MDL, Inc., San Leandro, CA, USA) suggested

commercially available sulfonyl and acid chlorides that could extend from the lead compound **1**. Sulfonyl chlorides and carbonyl chlorides selected included derivatives of aryl rings, heterocyclic rings (thiophene, oxazole, diazole), and condensed rings (naphthalene, quinoline, benzothio-phenene). When possible, substitutions were chosen to modulate the polarity of the inhibitors. The second, focused library was designed to explore the SAR of the highest affinity compound from the first library, using sequential liquid phase synthesis.

The first library of 28 compounds was synthesized using polymer-assisted liquid phase in-parallel chemistry at room temperature. 3-Aminophenylboronic acid hemisulfate was reacted with 28 different sulfonyl and carbonyl chlorides. Poly(4-vinylpyridine) resin (for amide derivatives) or (piperidinomethyl)-polystyrene resin (for sulfonamide derivatives) was used to scavenge the hydrochloric acid formed during the reaction. Aminomethylated polystyrene resin was added in a final step to scavenge the excess acid chloride [23]. The resins were filtered off and the filtrate concentrated under vacuum to give the final compounds. The second group of 12 compounds was synthesized through multi-step liquid phase chemistry. The final products were typically isolated through extraction with organic solvents; several were further purified by column chromatography.

3. Results

Initial modeling suggested that derivatives of **1** would bind in the R1 cleft, interacting with Leu119, Gln120 and



Scheme 1. In-parallel synthesis of 3-sulfonamide- and 3-amidephenylboronic acids. For amide derivatives, poly(vinylpyridine) resin was used as base.

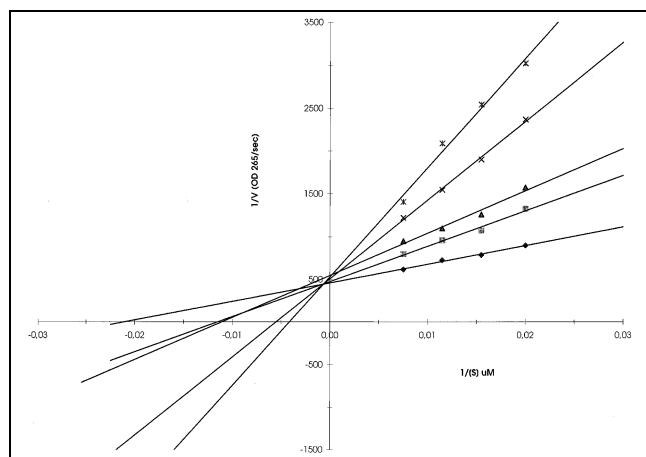


Fig. 3. Lineweaver–Burk plot of the inhibition of AmpC by compound **2**. Inhibitor concentrations were: 0 μM (\blacklozenge), 25 μM (\blacksquare), 50 μM (\blacktriangle), 100 μM (\times), and 200 μM (\ast). The K_i value is 83 nM.

Asn152 [9]. Compound **1** was derivatized by carbonyl and sulfonyl chlorides using polymer-assisted liquid phase in-parallel chemistry, resulting in 28 amide and sulfonamide derivatives (Scheme 1). The K_i values of these compounds ranged from 0.083 to 25 μM (Table 1). The sulfonamides typically had lower (better) K_i values than the amides. With few exceptions, the sulfonamides had K_i values less than 2 μM , whereas the K_i values of the amides ranged from 3 to 25 μM . Larger molecules with aromatic rings linked together linearly (e.g., **2** and **4**) typically had lower K_i values than did fused ring systems of about the same hydrophobicity (e.g., **6** and **9**). The most potent compound of this first series, **2**, inhibited AmpC competitively with a K_i value of 83 nM by full kinetic analysis (Fig. 3). For most inhibitors, K_i values were determined using progress curves, which are accurate for boronic acid inhibitors of group I β -lactamases [9,24].

Compound **2** was fit into the AmpC cleft using flexible ligand docking [22]. A total of 1584 orientations, each of which had 500 conformations, were evaluated for steric and electrostatic complementarity to the enzyme [25]. In the highest scoring orientation, the boronic acid of **2** hydrogen bonds with the main chain nitrogens of Ser64 and Ala318, the main chain oxygen of Ala318, and the hydroxyl of Tyr150 (Fig. 4). These interactions are highly con-

Table 3
Selectivity of **2** for AmpC versus serine proteases

Enzyme	IC_{50} ^a
AmpC	0.15
Chymotrypsin	30
Trypsin	> 100 ^b
Elastase	> 100 ^b

^aThe substrate to K_m ratio for AmpC was 2.5, with a K_m value of 40 μM [9]. The substrate to K_m ratio for chymotrypsin was 3.4, with a K_m value of 58 μM [47]. The substrate to K_m ratio for trypsin was 4, with a K_m value of 50 μM [48]. The substrate to K_m ratio for elastase was 0.1, with a K_m value of 6.2 mM [49]. See Section 6 for more details.

^bNo inhibition was observed at 25 μM . The values given for the IC_{50} assume that inhibition was no greater than 20% at this concentration.

served among β -lactamase–boronic acid complexes [8,10–13], and the calculation was biased toward them. In the docked orientation, the first phenyl ring of **2** forms a dipole–quadrupole interaction with the side chain amide of Asn152 (its N δ 2 atom comes as close as 2.9 \AA to the inhibitor ring). The sulfonamide nitrogen of **2** forms a dipole–quadrupole interaction with the aryl ring of Tyr221. The bridging thiophene ring is oriented toward the surface of the R1 cleft. The last, distal ring of the inhibitor appears to interact with Arg204. From the docked orientation, it seemed that larger derivatives of **2** might fit into the R1 cleft to better interact with residues such as Arg204 and the ‘omega loop’ [26] of AmpC, including residues Val211 and Ser212.

To explore the SAR of sulfonamides resembling **2**, 12 further compounds were synthesized using sequential liquid phase chemistry (Scheme 2). These compounds were designed to be more soluble and to interact with residues suggested by the docked conformation of **2**. Each of these compounds had a K_i of 1.2 μM or better. The most potent of them, **33**, had a K_i value of 60 nM (Table 2).

Boronic acids are known to inhibit serine proteases, and it seemed sensible to investigate the selectivity of the new inhibitors for AmpC. Compound **2** was 200-fold more active against AmpC than it was against chymotrypsin, and it was three orders of magnitude more selective for AmpC than it was against trypsin or elastase (Table 3).

Compounds **2** and **33** were tested in bacterial culture for their ability to reverse the resistance of β -lactamase-expressing bacteria to penicillins. At a concentration of

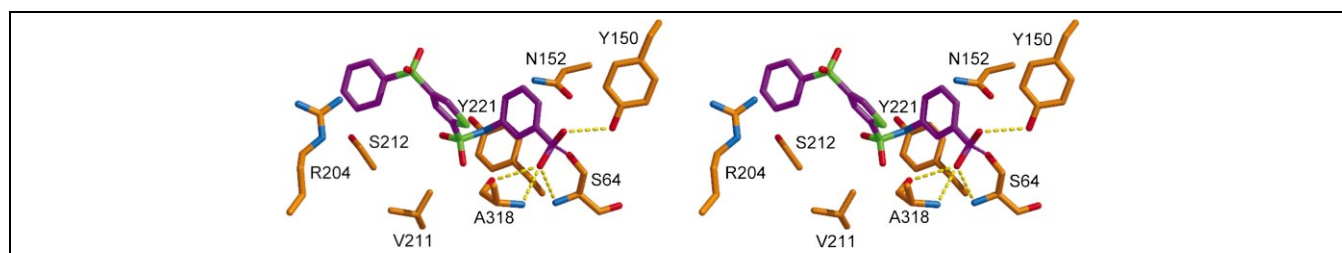


Fig. 4. The highest scoring docked orientation of **2** with AmpC. Dashed yellow lines indicate hydrogen bonds. The catalytic serine residue (S64) has been mutated to a glycine for the docking calculation (see Section 6). Carbon atoms of AmpC are colored orange, carbon atoms of **2** magenta, nitrogen atoms blue, oxygen atoms red, and sulfur atoms green.

Table 4
MICs^a for compounds **2** and **33**

Bacterium	Amx	2 alone	33 alone	Clav alone	Amx- 2 ^b	Amx- 33 ^b	Amx-Clav ^c
<i>S. epidermidis</i> 30995	64	256	64	32	8	4	2
<i>S. epidermidis</i> 31091	32	256	64	64	4	4	2
<i>S. aureus</i> 12	64	512	512	4	8	8	0.5
<i>S. aureus</i> 39	64	512	256	8	4	4	0.5
<i>S. aureus</i> 42	256	256	512	> 256	16	16	16
<i>S. aureus</i> 44	128	512	256	16	4	4	1
<i>S. epidermidis</i> 1108	128	256	512	8	4	8	0.5
<i>Micrococcus</i> sp. 3110925	256	128	128	> 256	16	8	32
<i>Bacillus</i> sp. 70002	8	256	256	256	2	4	4
<i>Nocardia</i> sp.	> 512	1024	512	> 256	128	256	64

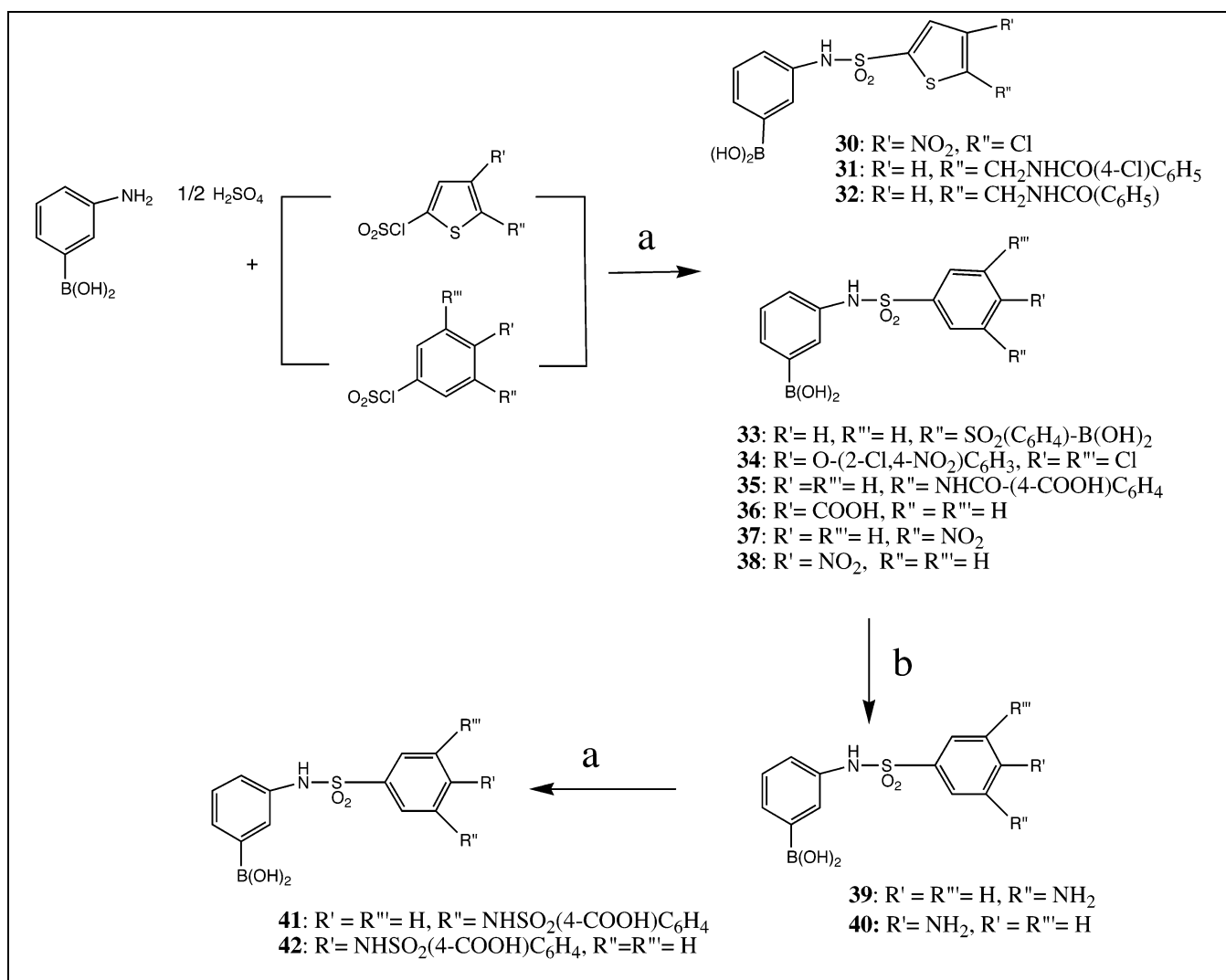
^aMIC in $\mu\text{g/ml}$; Amx: amoxicillin; Clav: clavulanic acid.

^bAmx/inhibitor = 1/3 (w/w).

^cAmx/Clav = 2/1 (w/w).

23.8 $\mu\text{g/ml}$ (50 μM), compound **33** potentiated the activity of ampicillin (200 $\mu\text{g/ml}$) against the JM109 strain of *Escherichia coli* expressing AmpC. However, against clinical isolates of Gram-negative bacteria, the inhibitors showed

little effect. Both inhibitors were active against Gram-positive strains thought to express group II β -lactamases. The inhibitors reduced the minimum inhibitory concentration (MIC) of amoxicillin by 8–32-fold against these bacteria,



Scheme 2. Sequential synthesis of focused library. (a) NaHCO_3 , pH 10, 4 N NaOH. (b) $\text{H}_2\text{O}/\text{MeOH}$, Pd/C 10%, H_2 2 atm.

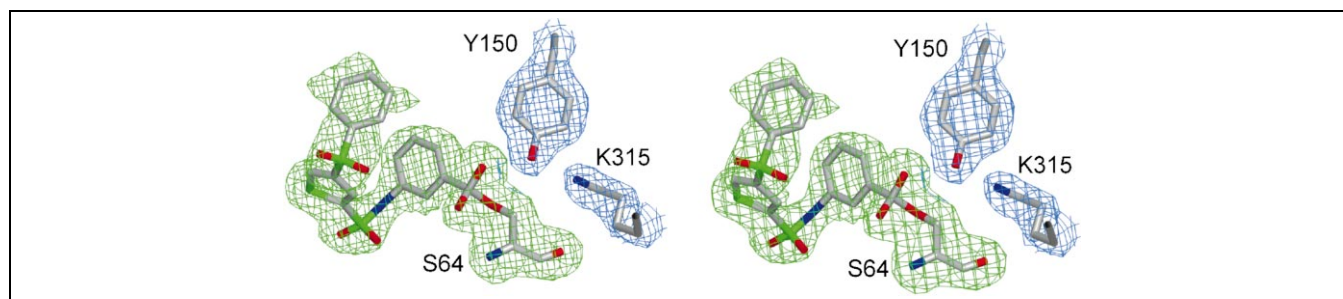


Fig. 5. Stereo view of electron density of the refined model of **2** in complex with AmpC. A $2F_o - F_c$ electron density map is represented by the blue cage and is contoured at 1.3σ . A simulated-annealing omit map of the inhibitor covalently attached to S64 is represented by the green cage and is contoured at 3.0σ . Atoms are colored as in Fig. 4, except all carbon atoms are colored gray. This figure was generated using SETOR [51].

typically to 4–16 $\mu\text{g/ml}$ (Table 4). Consistent with this observation, compounds **2**, **33**, and **41** inhibited PC1 β -lactamase from *Staphylococcus aureus* with K_i values in the 2–6 μM range (Table 5). Compounds **33** and **41** were also found to have micromolar K_i values versus the group II β -lactamase TEM-1 (Table 5).

To understand in detail how **2** interacted with AmpC, co-crystals of the enzyme/inhibitor complex were grown. The crystal diffracted to 2.7 \AA resolution on a rotating anode source, and difference electron density maps calculated from this data set verified the presence of the inhibitor in the active site (Table 6). Refinement was begun using this data set, and the inhibitor was modeled into the active site. Subsequently, the same crystal showed an improved diffraction limit at the Advanced Photon Source, Argonne National Laboratory, allowing the struc-

ture to be determined and refined to 2.1 \AA resolution (Table 6). The location and conformation of the inhibitor was clear in the initial $F_o - F_c$ difference electron density maps at 2.1 \AA resolution, contoured at 3.0σ , allowing it to be immediately added to the model. Following refinement, a simulated annealing omit map of the inhibitor was calculated and showed unambiguous positive difference density for the inhibitor (Fig. 5). As expected, greater detail was observed in the 2.1 \AA structure; this included several water molecules interacting with the inhibitor that were not observed in the 2.7 \AA structure. Other than the water structure, few changes were observed between the structure determined to 2.7 \AA and that determined to 2.1 \AA .

The quality of the final model for the 2.1 \AA structure was evaluated with the program Procheck [27]; 90.1% of

Table 5
 K_i values against other β -lactamase enzymes

inhibitor	structure	<i>S. aureus</i> PC1 K_i (μM)	TEM-1 K_i (μM)	<i>E. cloacae</i> P99 K_i (μM)
2		6	58.1	0.25
33		3.2	7.3	0.45
41		2	2.5	0.17

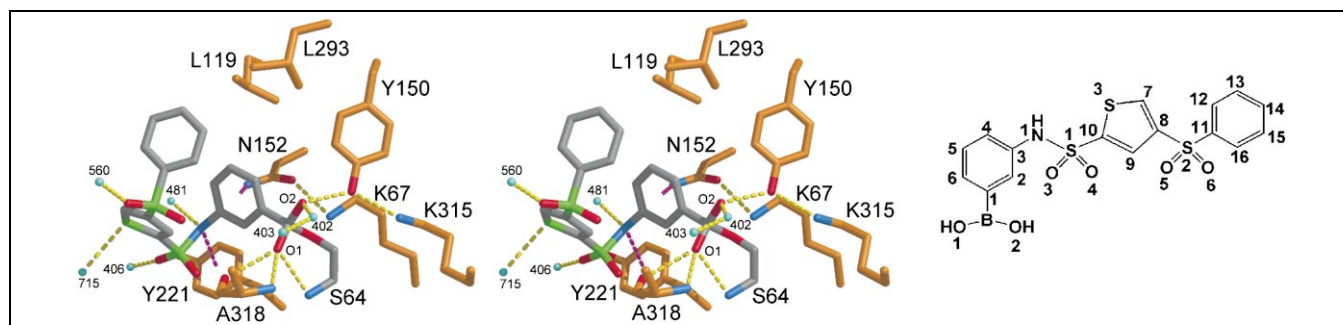


Fig. 6. Stereo view of key interactions observed in the complex of **2** with AmpC. Dashed yellow lines indicate hydrogen bonds. Dashed magenta lines indicate dipole–quadrupole interactions. Cyan spheres represent water molecules. Interaction distances, including distances from **2** to L119 and L293, are listed in Table 7. Atoms are colored as in Fig. 4, except the carbon atoms of the inhibitor are gray.

the non-glycine and non-proline residues were in the most favored regions of the Ramachandran plot, and the remaining residues were in the additionally allowed region. The final R and R_{free} values of the refined structure were 20.6% and 24.9%, respectively. This structure has been deposited in the PDB with accession code 1GA9.

In the crystallographic complex, **2** adopts a jack-knife structure, folding back upon itself so that the last phenyl ring of the inhibitor overlies the first phenyl ring, reducing the exposure of both to solvent (Fig. 6). The O_{γ} of Ser64 forms a dative covalent bond with the tetrahedral boronic acid. The $O1$ hydroxyl of the boronic acid hydrogen bonds with the main chain nitrogens of Ser64 and Ala318, and also with the main chain carbonyl oxygen of Ala318 (Table 7). The $O2$ hydroxyl hydrogen bonds with the putative catalytic base of AmpC, Tyr150 [14,15,28], and with a well-ordered water molecule (Wat402, Table 7). The first phenyl ring (i.e., the ring closest to Ser64) of the inhibitor

appears to form a dipole–quadrupole interaction with $N\delta 2$ of the key catalytic residue Asn152 (Fig. 6), consistent with interactions observed crystallographically with a small arylboronic acid [10]. The sulfonamide nitrogen ($N1$) of **2** forms a dipole–quadrupole interaction with the conserved Tyr221 aryl ring (Fig. 6), similar to interactions observed in the β -lactam loracarbef complex with AmpC [16]. $N1$ also interacts with a water molecule (Wat481). Another ordered water molecule (Wat406) interacts with a sulfonamide oxygen ($O4$, 2.9 Å), Tyr221OH (2.9 Å), Ser212O (2.6 Å), and Wat566 (2.9 Å). Up to this point, the crystallographic conformation of **2** closely overlies the docked structure (Fig. 7).

The major difference between the docked and the crystallographic structures results from a 165° rotation about the thiophene sulfone bond (i.e., $S1$ and $C10$ in Fig. 6), leading to a different placement of the final sulfonyl-phenyl group of the inhibitor. There are smaller conforma-

Table 6

Data collection and refinement statistics for the X-ray structures of the complex between compound **2** and AmpC, determined at 2.1 and 2.7 Å resolution

	2.1 Å resolution structure	2.7 Å resolution structure
Cell constants (Å; °)	$a = 118.99$ $b = 78.06$ $c = 97.79$; $\beta = 115.53$	$a = 119.10$ $b = 78.04$ $c = 97.87$; $\beta = 115.53$
Resolution (Å)	2.1	2.7
Unique reflections	42 312	20 295
Total reflections	156 406	69 949
R_{merge} (%)	7.3 (17.9) ^a	10.1 (34.5) ^a
Completeness (%)	89.8 (96.0) ^a	91.9 (98.4) ^a
$\langle I \rangle / \langle \sigma_I \rangle$	25.2	10.7
Resolution range for refinement (Å)	20–2.1 (2.18–2.10) ^a	20–2.7 (2.78–2.70) ^a
Number of protein residues	710	716
Number of water molecules	318	115
Rmsd bond lengths (Å)	0.013	
Rmsd bond angles (°)	1.651	
R -factor (%)	20.6	
R_{free} (%)	24.9 ^b	
Average B -factor, protein atoms (Å ²)	42.2 ^c	
Average B -factor, protein atoms (Å ² , A monomer only)	38.5	
Average B -factor, inhibitor atoms (Å ²)	60.2 ^c	
Average B -factor, inhibitor atoms (Å ² , A monomer only)	50.4	

^aValues in parentheses are for the highest resolution shell used in refinement.

^b R_{free} was calculated with 5% of reflections set aside randomly.

^cValues cited were calculated for both molecules in the asymmetric unit.

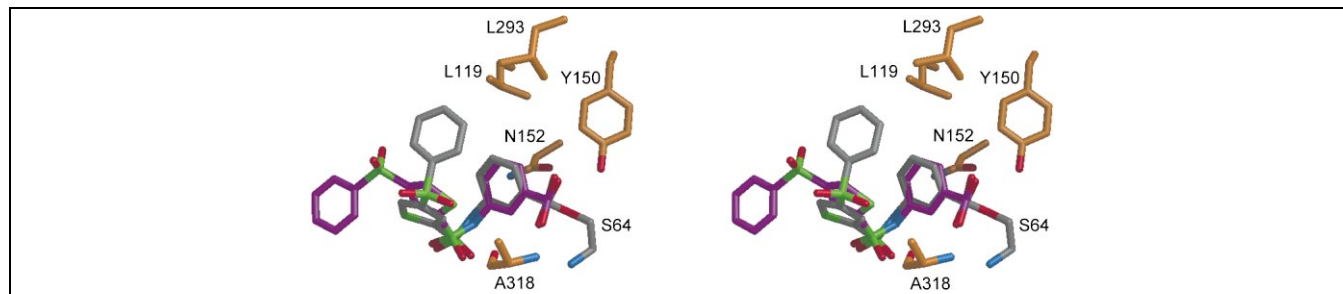


Fig. 7. Overlay of the docked and crystallographic conformations of **2** in the AmpC site. Atoms are colored as in Fig. 4, except carbon atoms of the docked inhibitor are magenta, and carbon atoms of the inhibitor in the crystal structure are gray.

tional changes about the thiophene ring bond with the second sulfone, and about the sulfone and the final phenyl ring. These rotations result in the distal sulfone forming a hydrogen bond between O6 of the inhibitor and Wat560 and the distal phenyl ring interacting with the conserved amino acids Leu119 and Leu293 (Table 7, Fig. 6).

4. Discussion

The R1 cleft of AmpC β -lactamase is an intriguing target for inhibitor design. The region is well defined structurally and is lined by highly conserved amino acids (Fig. 2). Some of these residues, such as Asn152 and Ala318, are known to bind to the amide functionality at the proximal end of all β -lactam R1 side chains [14–16,29,30] (Fig. 1). Little is known about what role the rest of the R1 cleft might have in recognizing β -lactams or other molecules. To investigate the potential of the R1 cleft as a site for inhibitor discovery, we used guided in-parallel synthesis, followed by crystallographic structure determination of an enzyme–inhibitor complex. The resulting derivatives had K_i values two orders of magnitude better than the initial lead. Despite this improvement, it is clear that smaller molecules can be found that bind in the same affinity range [9]. Also, boronic acids simply bearing the side chains of β -lactams [31] have been described that bind in the low nanomolar range to the group II β -lactamase TEM-1 [11] and in the 20–200 nM range to AmpC [12], and small aryl boronic acids that bind in the 500 nM range have been found for the group I β -lactamase from *Pseudomonas* [31]. What is unusual about the inhibitors and structures described here is the rapid elaboration of novel and disparate chemical functionality through guided in-parallel synthesis and the recognition of that functionality by the R1 cleft of AmpC.

Compound **2** makes several interactions with AmpC that are common to the small boronic acid inhibitors [10,13] (our unpublished results), and to a lesser extent a phosphonate inhibitor, in the ‘oxyanion’ [15] or ‘electrophilic’ [13] hole of the enzyme. Both the O1 and O2 hydroxyls of the inhibitor hydrogen bond with conserved catalytic residues of AmpC [10] (Fig. 6). The first phenyl

ring of the inhibitor (that closest to the bound boronic acid) appears to form dipole–quadrupole interactions with the key catalytic residue Asn152 [10] (Fig. 6).

New interactions are observed beyond the first phenyl-boronic acid. The dipole–quadrupole interaction between Tyr221 and the sulfonamide nitrogen of **2** mimics a similar interaction observed between this residue and the amino group of the substrate loracarbef [16]. Tyr221 is completely conserved among group I β -lactamases, but its

Table 7
Interactions in the crystallographic complex between **2** and AmpC

Interaction	Distance (Å)	
	A monomer	B monomer
S64N-O1	2.9	2.7
A318N-O1	2.7	2.8
A318O-O1	2.8	2.8
Y150OH-O2	2.6	2.6
Wat402-O2	2.9	2.7
Y150OH-K315N ζ	2.9	2.9
Y150OH-S64O γ	3.0	2.9
Y150OH-K67N ζ	3.5	3.5
centroid ring 1-N152N δ 2	3.6	3.5
K67N ζ -A220O	2.8	2.9
K67N ζ -S64O γ	2.7	2.6
K67N ζ -N152O δ 1	2.7	2.6
Wat402-T316O γ 1	3.3	3.3
Wat402-Wat403	2.7	NP ^a
Wat403-N346O δ 1	2.6	NP
Wat403-R349N η 2	3.0	NP
N1-Wat481	2.8	NP
N1-centroid Y221	3.5	3.5
O4-Wat406	2.9	2.9
S3-Wat715	3.2	NP
O6-Wat560	2.7	NP
O5-N343N δ 2	3.4	3.2
O5-T319O	4.0	2.8
C14-L119C δ 2	3.8	5.1
C15-L293C δ 1	4.0	4.2

^aNot present.

function is unknown. This residue may commonly interact with polar or aromatic groups through quadrupolar interactions. The last phenyl ring of the inhibitor jack-knives back over the first phenyl ring, forming van der Waals interactions with Leu119 and Leu293 (Fig. 6). These residues form a hydrophobic patch on one side of the R1 cleft. Leu119 is completely conserved among group I β -lactamases, and Leu293 is mostly conserved – it is replaced by Phe or Met in a few enzymes. The role of these residues in substrate recognition, if any, is unknown. The structure of **2** suggests that molecules may be designed to take advantage of the exposed hydrophobic surface area of these leucines to improve inhibition.

The jack-knifed conformation of **2** helps to explain the SAR of this family of inhibitors. To adopt this conformation, tetrahedral linkages are required between the three aryl rings of the inhibitor. Planar linkages, as in amide bonds, would lead to an extended conformation of the inhibitor, resulting in clashes with the binding site. In the first series of 28 inhibitors, tetrahedral sulfonamides are more potent than planar amides, with the nine most potent compounds all carrying a sulfonamide group (compounds **2–10**, Table 1). Comparing compound **21** with **37** and compound **20** with **38**, the replacement of an amide by a sulfonamide improves affinity by 10-fold. Similarly, converting the second sulfonamide of **41** to an amide in **35** results in a seven-fold decrease in binding. On the other hand, an inversion of the nitrogen and sulfone positions within this second sulfonamide linkage (compound **33** versus **41**), which maintains the tetrahedral geometry, has little effect on binding.

The 500-fold range of inhibition values in this series suggests that specific contacts are being made with the enzyme and that inhibition cannot be explained solely by general, non-specific features of these inhibitors. Although larger derivatives are often more potent than the smaller ones, neither size nor hydrophobicity is sufficient to explain the binding activity among these molecules. For instance, compound **3** is one of the smaller, but also one of the better inhibitors (K_i 0.1 μ M). Indeed, the larger ligands, though the most potent, do not realize as much potency for their increase in size as one might have expected. This may owe to the lack of interactions observed in the middle (thiophene) region of compound **2** in its complex with AmpC. This middle region may simply serve as a spacer linking the first third of the inhibitors, which make important interactions with the enzyme, to the last third of the inhibitors, which also appear to make important interactions (i.e., with Leu119 and Leu293). More broadly, small changes in the linker type, position, and length affect activity significantly. Two of the most polar inhibitors, **33** and **41**, are also the most potent.

Boronic acids act as transition-state analogs for serine β -lactamases in general, and also for serine proteases. To investigate the spectrum of action, we measured the inhibition of three of the most active of the new inhibitors

against the group II β -lactamases PC1 from *S. aureus* and TEM-1, and against the group I β -lactamase P99 from *Enterobacter cloacae* (Table 5). The inhibitors are 100-fold less active against the group II enzymes, but nevertheless still bind in the low micromolar range, with the exception of compound **2** against TEM-1. The inhibitors bind in the range of 100–250 nM against P99, consistent with its high similarity to AmpC. To investigate specificity of these new inhibitors, compound **2** was tested against several serine proteases (Table 3), showing better than 200-fold selectivity versus chymotrypsin and better than 1000-fold selectivity versus trypsin and elastase, compared to AmpC.

Given the relatively good inhibition of compounds **2**, **33**, and **41**, their poor activity against pathogenic Gram-negative bacteria expressing group I β -lactamases was disappointing; small arylboronic acids with similar inhibition values are active against these bacteria [9,10]. This lack of activity of these larger inhibitors may reflect difficulties with outer membrane penetration, which is frequently a problem with antibiotics acting against Gram-negative bacteria. Consistent with this hypothesis, compounds **2** and **33** were active against several Gram-positive pathogens (Table 4), in line with the micromolar K_i values against the group II β -lactamases expressed by these bacteria (Table 5). Although the ability of these inhibitors to reverse resistance in bacteria such as *S. aureus* and *S. epidermidis* is encouraging, to have broad-spectrum activity it will be necessary to improve the ability of these inhibitors to penetrate Gram-negative bacteria.

The structure of **2** in complex with AmpC was determined to a resolution of 2.7 Å and subsequently to 2.1 Å, from the same crystal. What additional information did the higher resolution structure provide us with in our inhibitor design efforts? The conformation of the inhibitor is very similar (rmsd between inhibitor atoms is 0.66 Å), and it is observed to make the same interactions with the amino acids of AmpC in both structures. For example, the interactions made by the boronic acid hydroxyls, the quadrupole-dipole interactions with Asn152 and Tyr221, and the interaction of the terminal phenyl ring of **2** with the hydrophobic patch formed by Leu119 and Leu293 are maintained. The only significant difference between the two structures is in the water structure; several water molecules that interact with **2** are seen only in the higher resolution structure. Several investigators have argued that a knowledge of the ordered waters can be used in the design or elaboration of an inhibitor [32–34], and to this extent, the 2.1 Å structure is more informative than the 2.7 Å structure. Nevertheless, it is clear that most information in the 2.1 Å structure is captured in the 2.7 Å structure, as far as the inhibitor is concerned. Perhaps the greatest argument in favor of the higher resolution data is that we feel more confident about the model that we have fit for them. The final models do not themselves differ significantly.

We used a docked structure of **2** in AmpC to design the second library of inhibitors, since a crystallographic complex was not available at that time. Subsequently, the structure of the complex with compound **2** was determined by X-ray crystallography; it is appropriate to ask how well this predicted structure corresponded to the experimentally determined structure, and how useful the model was in predicting new compounds. The docked and crystallographic conformations of **2** resemble each other closely for most of the molecule (Fig. 7). A ring flip in the thiophene leads to a different placement of the last phenyl ring, with the docked structure extending into the distal region of the R1 cleft and the crystallographic structure folding back upon itself in the proximal region of the cleft. As in previous studies, the docking program was able to predict the placement of the inhibitor to 'low resolution' [35–37]. Most of the inhibitor is correctly placed, but several key interactions are missed, probably owing to under-sampling conformations in the docking calculations.

How useful was the docked prediction in designing the second library of inhibitors? Both the docked structure and the SAR in this series suggested that tetrahedral sulfonamides would do better than planar amides, which led us to focus on the former in the second library. The docked structure properly suggested that the central thiophene of **2** functioned as a linker, making few interactions on its own, and could be replaced with more synthetically tractable groups, such as the phenyl ring used in most compounds in the second library. On the other hand, our failure to predict the placement of the last phenyl ring led to derivatives that were designed to complement the polar, distal part of the R1 cleft, as opposed to the hydrophobic patch made up of Leu119 and Leu293. Had the crystallographic complex of **2** with AmpC been available, we would have explored different derivatives, especially in the distal portion of the inhibitors, in the second library.

This said, the combination of structure-based design with in-parallel synthesis allowed for the rapid exploration of novel inhibitor functionality in the R1 cleft of AmpC. The crystallographic complex of the 83 nM inhibitor **2** is a guide to recognition in this cleft and a template for further design against AmpC β -lactamase. The unusual dipole–quadrupole interaction with the completely conserved Asn152 seems to be a conserved feature in arylboronic acids. In some ways this is surprising, since the same asparagine donates a hydrogen bond to the R1 amide carbonyl of β -lactams. Aryl rings are not typically considered good replacements for carbonyl oxygens, but in arylboronic acids this appears to be a critical contribution to the affinity [9,10]. The dipole–quadrupole interaction between the sulfonamide nitrogen and Tyr221 may be characteristic of this residue [10,16]. Similarly, the role of the exposed, conserved Leu119 and Leu293 in substrate recognition is not understood at this time. The interaction of these residues with the last phenyl ring of **2** suggests that,

irrespective of what these residues may contribute to β -lactam recognition, they can be used in the design of non- β -lactam inhibitors of AmpC.

5. Significance

Group I β -lactamases are a major cause of antibiotic resistance to β -lactams such as penicillins and cephalosporins. Known β -lactam-based inhibitors of β -lactamases have little effect on these enzymes, which are increasingly prevalent in hospital pathogens. To investigate potential complementarity of inhibitors for an open binding cleft observed in the structure of AmpC, a combination of structure-based design and in-parallel synthesis was adopted. This led to inhibitors with a 100-fold better affinity than the lead compound, exploring a wide range of derivatives. Several of these inhibitors reversed the resistance of Gram-positive bacteria, although they were much less effective against β -lactam-resistant Gram-negative bacteria. The crystal structure of an 83 nM inhibitor, in complex with the group I β -lactamase AmpC, suggests recognition roles for residues in the enzyme that are highly conserved but for which no function had previously been detected. This structure may serve as a template for future design in this series.

6. Materials and methods

6.1. Synthetic chemistry

3-Aminophenylboronic acid hemisulfate was purchased from Aldrich. Sulfonyl and carbonyl chlorides were purchased from Aldrich, Maybridge International, TCI-US, Lancaster, Fluka, and Asinex. (Piperidinomethyl)-polystyrene (2.6 mmol base/g resin; crosslinked with 2% divinyl-benzene (DVB); 200–400 mesh) and poly(4-vinylpyridine) (8.8 mmol base/g resin; crosslinked with 2% DVB; 60 mesh) resins were purchased from Fluka. Aminomethylated polystyrene (1.33 mmol base/g resin) was purchased from Novabiochem.

Liquid phase in-parallel synthesis was carried out on a 10-position platform shaker. The catalytic hydrogenation was accomplished using a stirred Reactor 'Parr', Mod.4561 3000 psi Magnetic Drive T316 Stainless Steel 230 V 50/60 Hz Air Motor.

The purity of all synthesized compounds was determined by thin layer chromatography (TLC) and by elementary analysis. For TLC, pre-coated silica gel 60 F₂₅₄ plates (Merck) were used. The plates were viewed using a UV/visible lamp at 254 nm and 366 nm. Silica gel (60M; 230–400 mesh, ASTM) was used for column chromatography. Elementary analyses were carried out in the microanalysis laboratory of the Dipartimento di Scienze Farmaceutiche, Modena University. Analyses were within $\pm 0.4\%$ of the theoretical values. All compounds were analyzed by one-dimensional ¹H NMR on Bruker AC200 and Bruker MX400 WB spectrometers (Centro Interdipartimentale Grandi

Strumenti, Modena University). Several compounds were also characterized through two-dimensional ^1H NMR. Unless otherwise stated, spectra were recorded in $\text{DMSO-}d_6$. Chemical shifts are reported in ppm from tetramethylsilane as internal standard.

6.2. Polymer-assisted liquid phase in-parallel chemistry

6.2.1. Synthesis of 3-acylamino- and 3-sulfonylaminophenylboronic acid derivatives using aminomethylated polystyrene resin as a scavenger (Compounds 2–29)

The syntheses were carried out in liquid phase in parallel (Scheme 1). For the synthesis of a single compound, 0.030 g (0.161 mmol) of 3-aminophenylboronic acid hemisulfate was suspended in anhydrous chloroform (CHCl_3 ; 6 ml), and the mixture was stirred at room temperature. Poly(4-vinylpyridine) resin (3 eq., 0.483 mmol; 8.8 mmol/g; 0.054 g) or (piperidinomethyl)-polystyrene resin (3 eq., 0.483 mmol; 2.6 mmol/g; 0.186 g) for amide or sulfonamide derivatives, respectively, was then added to the stirring mixture as scavenger. Different acid chlorides and sulfonyl chlorides (R-COCl or $\text{R-SO}_2\text{Cl}$, 1.5 eq., 0.241 mmol) were added to each batch, and the reactions were stirred until disappearance or great reduction of starting materials (reaction time 12–24 h). In the latter case, it was necessary to isolate the final product from starting materials. This procedure is described below for compounds 2–9, 12, 13, 21–24, 26, 27. Aminomethylated polystyrene resin (3 eq., 0.483 mmol; 1.33 mmol/g; 0.363 g) was added to the stirring mixture to scavenge the excess carbonyl or sulfonyl chloride and stirring was maintained for 4–5 h [23]. The resins were filtered off and the filtrate concentrated under vacuum to give the final 3-acylamino- or 3-sulfonylaminophenylboronic acid derivative.

TLC analysis of the reaction mixtures of compounds 2 and 4 showed presence of starting materials. The expected products were then purified through column chromatography (silica gel 60M; 230–400 mesh ASTM eluent system $\text{CH}_2\text{Cl}_2/\text{CH}_3\text{OH}$; 9:1).

TLC analysis of the reaction mixtures of compounds 3, 5–7, 9, 12, 13, 21–23, and 26 showed the presence of unreacted 3-aminophenylboronic acid. The desired products were separated as follows. The reaction mixture was treated with 4 N hydrochloric acid and then extracted three times with dichloromethane (CH_2Cl_2). The combined organic layers, containing the desired product, were dried over sodium sulfate (Na_2SO_4), filtered, and concentrated under vacuum. The collected product was then triturated and washed with ethyl ether.

TLC analysis of the reaction mixture of compounds 8, 24, and 27 showed the presence of the starting chloride, which was not completely scavenged by the aminomethylated polystyrene resin, and unreacted 3-aminophenylboronic acid. The reaction mixture was therefore treated with 4 N NaOH and then extracted with dichloromethane (CH_2Cl_2). The combined organic layers were dried over Na_2SO_4 , filtered, and concentrated under vacuum to reduce the volume. The same organic phase was then treated as described above for compounds 3, 5–7, 9, 12, 13, 21–23, and 26. Compounds 2, 3, and 4 were also synthesized through traditional liquid phase synthesis in larger amounts (see below). Purity and

Table 8
Purities and yields for compounds synthesized in parallel

Compound	Purity (%)	Chloride (eq.) ^a	Yield (%)
2	98	1.5	24
3	60	3	32
4	80	1.5	1
5	90	3	13
6	90	3	6
7	60	1.5	5
8	80	3	8
9	70	3	21
10	80	3	14
11	60	1.5	13
12	70	3	8
13	70	1.5	6
14	80	1.5	47
15	70	1.5	9
16	70	4.5	8
17	70	3	18
18	80	3	21
19	70	1.5	70
20	80	1.5	38
21	70	1.5	7
22	70	1.5	13
23	90	1.5	28
24	70	3	9
25	90	3	38
26	80	1.5	18
27	70	3	4
28	70	1.5	42
29	70	1.5	10

^aMolar equivalent chloride used for the synthesis.

yields of compounds synthesized in parallel, as well as elementary analysis data, are available in Tables 8 and 9.

6.3. Liquid phase synthesis

6.3.1. 3-(4-Benzenesulfonyl-thiophene-2-sulfonylamino)-phenylboronic acid (2)

0.3 g (1.61 mmol) of 3-aminophenylboronic acid hemisulfate (1) was dissolved in sodium bicarbonate (0.5 M NaHCO_3 , 30 ml) followed by pH adjustment to 10 using sodium hydroxide (4 N NaOH). The solution, kept under stirring at room temperature, was then added to the 4-(benzenesulfonyl)-thiophene-2-sulfonyl chloride (1.5 eq.; 2.415 mmol, 0.779 g) already dissolved in acetone (10 ml). After stirring overnight, the solution was acidified with hydrochloric acid (4 N HCl) and extracted with dichloromethane (CH_2Cl_2) three times. The combined organic layers were dried over sodium sulfate (Na_2SO_4) and the solvent removed under vacuum. The collected crude product was then crystallized from acetone/petroleum ether 60:80. Yield: 0.163 g, 24%.

^1H NMR (DMSO) δ 7.17 (1H, dd, H-3), 7.29 (1H, t, H-2), 7.65 (1H, d, H-1), 7.73 (2H, t, H-8, H-10), 7.61 (1H, s, H-4), 8.75 (1H, s, H-6), 7.78 (1H, s, H-5), 7.83 (1H, t, H-9), 8.17 (B(OH)₂, s), 9.00 (2H, d, H-7, H-11), 10.54 (NH₂SO₂, s). Cosy correlation: H1–H2, H2–H3, H3–H4, H7–H8, H8–H9.

Table 9
Elementary analysis data for selected compounds

Compound	Formula	MW	C%	H%	N%	
2^a	C ₁₆ H ₁₄ NO ₆ S ₃ B	423.30	45.40	3.34	3.31	% calc
			45.44	3.36	3.30	% found
3^a	C ₁₁ H ₁₃ N ₂ O ₅ SB	296.12	44.62	4.43	9.46	% calc
			44.74	4.44	9.43	% found
4^a	C ₁₆ H ₁₄ NO ₆ S ₃ B	423.30	45.40	3.34	3.31	% calc
			45.58	3.23	3.32	% found
30	C ₁₀ H ₈ N ₂ O ₆ S ₂ BCl	362.58	33.12	2.23	7.73	% calc
			33.21	2.21	7.75	% found
31	C ₁₈ H ₁₆ N ₂ O ₅ S ₂ ClB	450.74	47.96	3.59	6.22	% calc
			47.80	3.60	6.24	% found
32	C ₁₈ H ₁₇ N ₂ O ₅ S ₂ B	416.29	51.93	4.12	6.73	% calc
			52.05	4.15	6.70	% found
33	C ₁₈ H ₁₈ N ₂ O ₈ S ₂ B ₂	476.11	45.40	3.82	5.89	% calc
			45.54	3.84	5.92	% found
34	C ₁₈ H ₁₂ N ₂ O ₇ SBCl ₃	517.54	41.77	2.34	5.41	% calc
			41.63	2.35	5.38	% found
35	C ₂₀ H ₁₇ N ₂ O ₇ SB	440.25	54.56	3.90	6.36	% calc
			54.38	3.88	6.37	% found
36	C ₁₃ H ₁₂ NO ₆ SB	321.13	48.62	3.77	4.63	% calc
			48.80	3.75	4.62	% found
37	C ₁₂ H ₁₁ N ₂ O ₆ SB	322.12	44.74	3.45	8.70	% calc
			44.58	3.44	8.68	% found
38	C ₁₂ H ₁₁ N ₂ O ₆ SB	322.12	44.74	3.45	8.70	% calc
			44.81	3.47	8.72	% found
39	C ₁₂ H ₁₃ N ₂ O ₄ SB	292.13	49.33	4.49	9.59	% calc
			49.49	4.52	9.61	% found
41	C ₁₉ H ₁₇ N ₂ O ₈ S ₂ B	476.30	47.91	3.60	5.88	% calc
			48.02	3.60	5.91	% found
42	C ₁₉ H ₁₇ N ₂ O ₈ S ₂ B	476.30	47.91	3.60	5.88	% calc
			47.73	3.57	5.85	% found

^aCompound was resynthesized and purified as described in Section 6.

6.3.2. 3-(3,5-Dimethyl-isoxazole-4-sulfonylamino)-phenylboronic acid (**3**)

0.2 g (1.075 mmol) of 3-aminophenylboronic acid hemisulfate (**1**) was dissolved in sodium bicarbonate (0.5 M NaHCO₃, 20 ml) followed by pH adjustment to 10 using sodium hydroxide (4 N NaOH). The solution, kept under stirring at 30°C, was then added to the 3,5-dimethyl-isoxazole-4-sulfonyl chloride (1.5 eq.; 1.61 mmol, 0.315 g) already dissolved in acetone (10 ml) [52]. After stirring 4–5 h, the insoluble portion was filtered off, and the clear solution was acidified with hydrochloric acid (4 N HCl) and extracted with ethylacetate three times (15 ml each). The combined organic layers were dried over sodium sulfate (Na₂SO₄) and the solvent removed under vacuum. The collected product was then triturated with ethyl ether. Yield: 0.124 g, 39%.

¹H NMR (DMSO) δ 2.18 (CH₃, s), 2.29 (CH₃, s), 7.20 (1H, d, H-3), 7.37 (1H, t, H-2), 7.62 (1H, d, H-1), 7.69 (1H, s, H-4), 8.11 (B(OH)₂, s), 10.35 (NHSO₂, s).

6.3.3. 3-(5-Benzenesulfonyl-thiophene-2-sulfonylamino)-phenylboronic acid (**4**)

Compound **4** was prepared according to the method described for **3** starting from 0.2 g (1.075 mmol) of **1** and 5-benzenesulfonyl-thiophene-2-sulfonyl chloride (1.5 eq.; 1.61 mmol, 0.521 g). Yield: 0.140 g, 31%.

¹H NMR (DMSO) δ 7.23 (1H, dd, H-3), 7.35 (1H, t, H-2), 7.59 (2H, d, H-5, H-6), 7.66 (1H, d/o, H-1), 7.66 (1H, d/o, H-4), 7.76 (1H, t/o, H-8), 7.79 (1H, t, H-9), 7.90 (2H, d, H-5, H-6), 8.29 (B(OH)₂, s), 8.60 (1H, d, H-7), 10.69 (NHSO₂, s). Cosy correlation: H1–H2, H2–H3, H3–H4, H5–H6, H7–H8, H8–H9.

6.3.4. 3-(5-Chloro-4-nitro-thiophene-2-sulfonylamino)-phenylboronic acid (**30**)

Compound **30** was prepared according to the method described for **3** starting from **1** (0.2 g, 1.075 mmol) and 5-chloro-4-nitro-thiophene-2-sulfonyl chloride (0.423 g, 1.5 eq.). The final crude product, 0.144 g, was purified by column chromatography using CH₂Cl₂/CH₃OH 9:1 as eluent. Yield: 0.08 g, 21%.

¹H NMR (DMSO) δ 7.32 (1H, dd, H-3), 7.41 (1H, t, H-2), 7.67 (1H, d/o, H-1), 7.67 (1H, s/o, H-4), 7.72 (1H, s, H-5), 7.99 (B(OH)₂, s), 10.8 (NHSO₂, s).

6.3.5. 3-{5-[(4-Chloro-benzoylamino)-methyl]-thiophene-2-sulfonylamino}-phenylboronic acid (**31**)

Compound **31** was prepared according to the method described for **3** starting from **1** (0.1 g, 0.54 mmol) and 5-(4-chloro-benzoylamino)-methyl-thiophene-2-sulfonyl chloride (0.282 g, 1.5 eq.). The crude product, 0.240 g, was purified by column chromatography with CH₂Cl₂/CH₃OH 9:1 as eluent. Yield: 0.07 g, 27%.

¹H NMR (DMSO) δ 4.57 (CH₃, s), 7.09 (1H, d, H-6), 7.29

(1H, dd, H-3), 7.32 (1H, t, H-2), 7.45 (1H, d, H-5), 7.59 (1H, d/o, H-1), 7.59 (1H, s/o, H-4), 7.65 (2H, d, H-8, H-9), 7.95 (2H, d, H-7, H-10), 9.36 (CONH, t), 10.33 (NHSO₂, s).

6.3.6. 3-[5-[(Benzoylamino)-methyl]-thiophene-2-sulfonylamino]-phenylboronic acid (**32**)

Compound **32** was prepared according to the method described for **3** starting from **1** (0.1 g, 0.54 mmol) and 5-(benzoylamino)-methyl-thiophene-2-sulfonyl chloride (0.255 g, 1.5 eq.). Yield: 0.180 g, 80%.

¹H NMR (DMSO) δ 4.68 (CH₂, s), 5.57 (1H, s/o, H-4), 7.086 (1H, d, H-6), 7.28 (1H, d/o, H-3), 7.32 (1H, t, H-2), 7.45 (1H, d, H-5), 7.57 (1H, d/o, H-1), 7.65 (3H, m/o, H-8, H-9, H-10), 7.94 (2H, dd, H-7, H-11), 9.29 (NHCO, t), 10.32 (NHSO₂, s).

6.3.7. 3,3'-(1'',3''-Benzenedisulfonamide) phenylboronic acid (**33**)

Compound **33** was prepared according to the method described for **3** starting from **1** (0.141 g, 0.762 mmol) and 1,3-benzenedisulfonyl chloride (0.363 mmol 0.1 g). The final product was purified by column chromatography using CH₂Cl₂/CH₃OH 95:5 as eluent. Yield: 0.083 g, 64%.

¹H NMR (DMSO) δ 7.05 (2H, dd, H-3, H-3'), 7.24 (2H, t, H-2, H-2'), 7.57 (2H, d/o, H-1, H-1'), 7.57 (2H, s/o, H-4, H-4'), 7.76 (1H, t, H-6), 7.97 (1H, dd, H-5), 7.97 (1H, dd, H-7), 8.185 (1H, d, H-8), 8.86 (B(OH)₂, s), 10.40 (NHSO₂, s), 10.72 (SO₂NH, s).

6.3.8. 3-[3,5-Dichloro-4-(2-chloro-4-nitro-phenoxy)-benzenesulfonylamino]-phenylboronic acid (**34**)

Compound **34** was prepared according to the method described for **3** starting from **1** (0.08 g, 0.43 mmol) and 3,5-dichloro-4-(2-chloro-4-nitro-phenoxy)-benzenesulfonyl chloride (0.359 g, 2 eq.). The final crude product, 0.2 g, was purified by column chromatography using CH₂Cl₂/CH₃OH 9:1 as eluent. Yield: 0.090 g, 40%.

¹H NMR (DMSO) δ 6.78 (1H, d, H-7), 7.19 (1H, dd, H-8), 7.29 (1H, dd, H-3), 7.41 (1H, t, H-2), 7.55 (1H, d, H-9), 7.55 (1H, s, H-4), 7.69 (1H, d, H-1), 7.92 (2H, s, H-5, H-6), 10.43 (NHSO₂, s).

6.3.9. 3-[3-(4-Carboxy-benzoylamino)-benzenesulfonylamino]-phenylboronic acid (**35**)

Compound **35** was prepared according to the method described for **3** starting from **1** (0.15 g, 0.806 mmol) and 3-(4-carboxy-benzoylamino)-benzene sulfonyl chloride (1.21 g, 1.5 eq.). The crude product was purified by column chromatography using CH₂Cl₂/CH₃OH 9:1 as eluent. Yield: 0.06 g, 18%.

¹H NMR (DMSO) δ 7.26 (1H, d/o, H-3), 7.305 (1H, t, H-2), 7.57 (1H, d, H-1), 7.57 (1H, s/o, H-4), 7.81 (1H, t, H-6), 7.95 (2H, d, H-10, H-11), 8.01 (1H, d/o, H-7), 8.05 (2H, d, H-9, H-12), 8.28 (1H, d, H-5), 8.43 (1H, s, H-8), 10.35 (NHCO, s), 10.81 (NHSO₂, s).

6.3.10. 3-(4-Carboxy-benzenesulfonylamino)-phenylboronic acid (**36**)

Compound **36** was prepared according to the method described for **3** starting from **1** (0.1 g, 0.54 mmol) and 4-(chlorosulfonyl) benzoic acid (0.355 g, 3 eq.). Yield: 0.046 g, 27%.

¹H NMR (DMSO) δ 7.58 (1H, d/o, H-1), 7.22 (1H, dd, H-3), 7.30 (1H, t, H-2), 7.58 (1H, s/o, H-4), 7.93 (2H, d, H-6, H-7), 8.02 (B(OH)₂, s/o), 8.15 (2H, d, H-5, H-8), 10.45 (NHSO₂, s).

6.3.11. 3-(3-Nitro-benzenesulfonylamino)-phenylboronic acid (**37**)

Compound **37** was prepared according to the method described for **3** starting from **1** (0.2 g, 1.075 mmol) and 3-nitro-benzene sulfonyl chloride (0.357 g, 1.5 eq.). Yield: 0.180 g, 52%.

¹H NMR (DMSO) δ 7.23 (1H, dd, H-3), 7.32 (1H, t, H-2), 7.52 (1H, d, H-1), 7.59 (1H, s, H-4), 8.09 (B(OH)₂, s), 8.20 (1H, d, H-7), 8.53 (1H, d, H-5), 8.58 (1H, s, H-8), 9.94 (1H, t, H-6), 10.48 (NHSO₂, s).

6.3.12. 3-(4-Nitro-benzenesulfonylamino)-phenylboronic acid (**38**)

Compound **38** was prepared according to the method described for **3** starting from **1** (0.4 g, 2.15 mmol) and 4-nitro-benzene sulfonyl chloride (0.477 g, 1 eq.). Yield: 0.559 g, 81%.

¹H NMR (DMSO) δ 7.21 (1H, dd, H-3), 7.32 (1H, t, H-2), 7.55 (1H, d, H-1), 7.55 (1H, s/o, H-4), 8.04 (2H, d, H-6, H-7), 8.42 (2H, d, H-5, H-8), 10.53 (NHSO₂, s).

6.3.13. 3-(3-Amino-benzenesulfonylamino)-phenylboronic acid (**39**)

The starting nitro derivative (**37**) (0.1 g, 0.311 mmol) was dissolved in a mixture of water (30 ml) and methanol (10 ml). The catalyst Pd/C (13%, 0.013 g) was added to the solution, transferred to a reactor, and stirred under 2 atm of H₂ for 1 h [53]. At the end of the reaction, the catalyst was filtered off and the solution concentrated under vacuum, giving the pure reduced amino derivatives. Yield: 0.070 g, 77%.

6.3.14. 3-(4-Amino-benzenesulfonylamino)-phenylboronic acid (**40**)

The starting nitro derivative (**38**) (0.2 g, 0.311 mmol) was dissolved in a mixture of water (60 ml) and methanol (20 ml). The catalyst Pd/C (10%, 0.020 g) was then added to the solution, transferred to a reactor, and stirred under 2 atm of H₂ for 1 h [53]. The catalyst was then filtered off and the solution concentrated under vacuum, giving the reduced amino derivatives. Yield: 0.160 g, 88%.

¹H NMR (DMSO) δ 6.61 (2H, d, H-6, H-7), 7.21 (1H, dd/o, H-3), 7.27 (1H, t/o, H-2), 7.3 (NH₂, o), 7.43 (2H, d, H-5, H-8), 7.48 (1H, s/o, H-4), 7.50 (1H, d, H-1), 8.04 (B(OH)₂, s), 9.75 (NHSO₂, s).

6.3.15. 3-[3-(4-Carboxy-benzenesulfonylamino)-benzenesulfonylamino]-phenylboronic acid (**41**)

Compound **41** was prepared according to the method described for **3** starting from **39** (0.04 g, 0.137 mmol) and 4-carboxy-benzenesulfonyl chloride (0.045 g, 1.5 eq.). The final product, 0.015 g, was purified through column chromatography using CH₂Cl₂/CH₃OH 9:1 as eluent. Yield: 0.008 g, 12%.

¹H NMR (DMSO) δ 7.07 (1H, d, H-3), 7.20 (1H, t, H-2), 7.30 (1H, t/m, H-6), 7.46 (2H, d, H-5, H-7), 7.56 (1H, d, H-1), 7.59 (1H, s, H-4), 7.85 (1H, s, H-8), 7.87 (2H, d, H-9, H-12), 8.15 (2H, d, H-10, H-11), 10.05 (NHSO₂, s), 10.28 (NHSO₂, s), 10.98

(COOH, s). Cosy correlation: H1–H2, H2–H3, H3–H4, H5–H6, H8–H5, H8–H6, H8–H7, H9–H10.

6.3.16. 3-[4-(4-Carboxy-benzenesulfonylamino)-benzenesulfonylamino]-phenylboronic acid (**42**)

Compound **42** was prepared according to the method described for **3** starting from **40** (0.1 g, 0.343 mmol) and 4-carboxy-benzenesulfonyl chloride (0.113 g, 1.5 eq.). The final product, 0.143 g, was purified by column chromatography using CH₂Cl₂/CH₃OH 9:1 as eluent. Yield: 0.019 g, 12%.

¹H NMR (CD₃COCD₃) δ 7.32 (1H, d/o, H-3), 7.35 (1H, t, H-2), 7.46 (2H, d, H-6, H-7), 7.78 (1H, d/o, H-1), 7.78 (1H, s/o, H-4), 7.82 (2H, d/o, H-5, H-8), 8.073 (2H, d, H-10, H-11), 8.28 (2H, d, H-9, H-12), 8.92 (SO₂NH, s), 9.79 (NHSO₂, s).

6.4. Enzymology

Stock solutions of the inhibitors were made up in dimethylsulfoxide (DMSO) at 10 mM, and subsequent 10-fold or 100-fold stock dilutions were made into 50 mM potassium phosphate buffer, pH 7.0. Assay conditions for AmpC β-lactamase and P99 β-lactamase from *E. cloacae* were the same, as described [9]. The P99 enzyme was a gift from Sergei Vakulenko and was used without further purification. All reactions were initiated by enzyme in an HP8453 UV/visible spectrophotometer with multi-cell transport running HP ChemStation software (version 2.5). The hydrolysis of the substrates cephalothin (for AmpC) or furyl-acrylpenicillanic acid (FAP) (for PC1 β-lactamase) was monitored at 265 and 340 nm, respectively. For PC1 β-lactamase from *S. aureus* (a gift from Robert Bonomo), 50 mM potassium phosphate, pH 7.0 was used as a buffer. The concentration of enzyme in the assays was 3 × 10⁻⁴ mg/ml, based on dilution from the stock solution provided. Reactions were monitored in methacrylate cuvettes. The *K_m* of FAP for this enzyme was determined to be 8 μM, and this value was used in the determination of *K_i* values using the progress curve method [7,9]. For TEM-1, 50 mM potassium phosphate, pH 7.0 was used as buffer. The concentration of enzyme in the assays was 7.7 × 10⁻² μM. Reactions were monitored in methacrylate cuvettes. The *K_m* of FAP for TEM-1 was determined to be 17 μM, and this value was used in the determination of *K_i* values using the progress curve method [7,9]. The *K_m* values of cephalothin for AmpC and P99 were 40 μM and 11 μM, respectively, and these values were used to determine *K_i* values using progress curves [7,9]. Several compounds were tested for effects of pre-incubation, but none was noted, consistent with earlier studies [9,24].

For the Lineweaver–Burk analyses of **2**, initial reaction rates were calculated from fits to the time course of each reaction. At least three rate values for each substrate–inhibitor combination were determined. These values were averaged together and plotted (Fig. 3).

Inhibition assays against α-chymotrypsin, trypsin, and elastase were performed in conditions as described [12]. The substrates were: for chymotrypsin, *N*-benzoyl-L-tyrosine-ethyl-ester, 200 μM; for trypsin, *N*-benzoyl-L-arginine-ethyl-ester, 200 μM; for elastase MeOSuc-Ala-Ala-Pro-Val-pNA, 640 μM. All reactions were initiated with enzyme.

6.5. Molecular docking

Flexible ligand docking [22] was used to fit **2** into AmpC, using structure 1C3B [10] from the PDB. An ensemble of 500 low energy conformations of **2** was calculated using Sybyl (Tripos, St. Louis, MO, USA). The boron atom was replaced by an sp³ carbon, since the boron parameters were not present in the Sybyl database; the lengths of the B–O and B–C bonds were manually corrected based on the X-ray crystal structure of benzo(*b*)thiophene-2-boronic acid bound to AmpC [10]. A formal charge of –1 was assigned to the boronic acid group, consistent with its charge state in the adduct [13,38]; this charge was localized to the boronic oxygen atoms. Gasteiger–Marsili [39] charges were calculated for the other inhibitor atoms. All rotatable bonds were sampled in 120° increments, with the exception of the carbon–boron bond, which was not rotated, and the bond between the 3-amino and the phenyl ring, which was rotated in 60° increments [22].

In the docking calculation, pseudo-atom ‘spheres’ were created by merging atom positions of four inhibitors that had been previously crystallized with AmpC or the group I β-lactamase from *E. cloacae*. The inhibitors were 3-aminophenylboronic acid [13], 3-nitrophenylboronic acid (Powers and Shoichet, unpublished), benzo(*b*)thiophene-2-boronic acid [10], and *m*-carboxyphenyl ((*N*-((*p*-iodophenyl)acetyl)amino)methyl) phosphonate [15]. A total of 31 atoms from these structures were used as ‘spheres’. Critical spheres corresponding to the positions of the boronic hydroxyls from 3-nitrophenylboronic acid and benzo(*b*)thiophene-2-boronic acid were used to restrict the sampling of the site. Chemical labeling of these spheres [40] biased the docking to match the boronic acid moiety of **2** to these spheres. A distance tolerance of 1.2 Å was used for matching ligand atoms onto sphere positions; a maximum of five and a minimum of four atom–sphere overlaps were imposed to specify an orientation. To allow for a close, covalent approach between the O_γ of Ser64 and the boron atom of the inhibitor, the Cβ and O_γ atoms of the Ser were deleted from the structure of the enzyme. Steric fit was evaluated using a grid calculated by the program DISTMAP [40]; allowed polar and non-polar contacts were set to a minimum of 2.3 and 2.6 Å, respectively. Van der Waals interaction energies were calculated using grids from the program CHEMGRID [25] based on the AMBER potential [41]. Electrostatic interaction energies were calculated using grids from the program DelPhi [42]. Rigid body minimization was not used.

6.6. Crystal growth and structure determination

Co-crystals of **2** were grown by vapor diffusion in hanging drops equilibrated over 1.7 M potassium phosphate buffer (pH 7.0) using microseeding techniques. The initial concentration of protein in the drop was 95 μM, and the concentration of the inhibitor was 600 μM. The inhibitor was added to the crystallization drop in a 2% DMSO, 1.7 M potassium phosphate buffer (pH 7.0) solution. Crystals appeared after several months with equilibration at 23°C.

The 2.7 Å data set was collected on an R-Axis IIC image plate

system at -170°C . Data for the 2.1 Å structure were collected on the DND-CAT beam line (SIDB) of the Advanced Photon Source at Argonne National Lab at 100 K using a 162 mm Mar CCD detector. Prior to data collection, crystals were immersed in a cryoprotectant solution of 20% sucrose, 1.7 M potassium phosphate, pH 7.0, for about 20 s, then flash cooled in liquid nitrogen. Both the 2.1 Å and the 2.7 Å data sets were collected from the same crystal.

Reflections were indexed, integrated, and scaled using the HKL program suite [43] (Table 6). The space group was C2, with two AmpC molecules in the asymmetric unit. Each AmpC molecule contains 358 residues, but electron density for residues B43–45 and B202–204 of molecule 2 was not observed, so they were deleted from the model. The structure was determined by molecular replacement using an AmpC/boronic acid complexed structure [10], with inhibitor and water molecules removed, as the initial phasing model. The model was refined using the maximum likelihood target in CNS and included a bulk solvent correction and a sigma cutoff of 2.0 [44]. Sigma A-weighted electron density maps were calculated using CNS, and manual rebuilding was done in the program O [45]. The inhibitor was built into the observed difference density in each active site of the asymmetric unit, and the structure of the complex was further refined using CNS (Table 6). All atoms were refined with an occupancy of 1.0, with the exception of residues A172 and B293. These residues were observed in two conformations and were modeled as such, with all atoms of each residue having an occupancy of 0.5 for each of the conformations.

6.7. Bacteriology

Susceptibility testing was performed and interpreted following the guidelines of the National Committee for Clinical Laboratory Standards [46], with the exception of experiments performed with a laboratory strain of JM109 *E. coli*. To test the inhibitory activity of **2** and **33**, the compounds were dissolved in 50% DMSO, and dilutions were performed using growth medium. An adequate final concentration in which to determine the MIC was obtained where the concentration of DMSO was maintained below 5%. The MIC of amoxicillin, in the presence and absence of the boronic acids, was determined against several Gram-positive resistant clinical isolates from the Hospital Ramón y Cajal, Madrid, that show a group II β -lactamase phenotype (Table 4).

For susceptibility testing against a laboratory strain of JM109 *E. coli* expressing AmpC, **33** was dissolved in DMSO at a concentration of 10 mM and diluted into LB broth to 400 μM (<2% DMSO). Compound **33** had no effect on its own at this concentration. This solution was serially diluted into 1 ml volumes of LB that also contained 200 $\mu\text{g}/\text{ml}$ ampicillin. Each tube was then inoculated with 10 μl of a fresh overnight culture of JM109 *E. coli* expressing AmpC on a temperature-inducible plasmid. The cultures were incubated at 37°C overnight with shaking. The concentration of **33**, in combination with ampicillin, at which no growth was observed was determined visually.

Acknowledgements

We thank D. Lorber, S. McGovern, and R. Silverman for reading the manuscript; D. Freymann and P. Focia for help with X-ray crystallographic experiments and refinement; R. Bonomo for providing PC1 β -lactamase; S. Vakulenko for a gift of recombinant P99 β -lactamase; and D. Lorber for help with molecular docking. We also thank Dr. S. Ghelli for help with NMR experiments, R. Galesi of the Microanalyses Laboratory, and the Centro Interdipartimentale Grandi Strumenti (CIGS) of Modena University. This work was supported by NIH GM59957 (to B.K.S.); we thank MDL, Inc. (San Leandro, CA, USA) for use of the ACD database and ISIS. D.T. was partly supported by a postdoctoral fellowship from the Dipartimento di Scienze Farmaceutiche, Università di Modena e Reggio Emilia. The DuPont-Northwestern-Dow Collaborative Access Team at the APS is supported by E.I. DuPont de Nemours and Co., the Dow Chemical Company, the National Science Foundation, and the State of Illinois.

References

- [1] H.C. Neu, The crisis in antibiotic resistance, *Science* 257 (1992) 1064–1073.
- [2] F. Baquero, J. Blazquez, Evolution of antibiotic resistance, *Trends Ecol. Evol.* 11 (1997) 482–487.
- [3] R. Sutherland, Beta-lactamase inhibitors and reversal of antibiotic resistance, *Trends Pharmacol. Sci.* 12 (1991) 227–232.
- [4] C.C. Sanders, Beta-lactamases of gram-negative bacteria: new challenges for new drugs, *Clin. Infect. Dis.* 14 (1992) 1089–1099.
- [5] K. Bush, The evolution of beta-lactamases, *Ciba Found Symp.* 207 (1997) 152–163.
- [6] J. Davies, Inactivation of antibiotics and the dissemination of resistance genes, *Science* 264 (1994) 375–382.
- [7] T. Beesley, N. Gascoyne, V. Knott-Hunziker, S. Petursson, S.G. Waley, B. Jaurin, T. Grundstrom, The inhibition of class C beta-lactamases by boronic acids, *Biochem. J.* 209 (1983) 229–233.
- [8] N.C. Strynadka, R. Martin, S.E. Jensen, M. Gold, J.B. Jones, Structure-based design of a potent transition state analogue for TEM-1 beta-lactamase, *Nature Struct. Biol.* 3 (1996) 688–695.
- [9] G.S. Weston, J. Blazquez, F. Baquero, B.K. Shoichet, Structure-based enhancement of boronic acid-based inhibitors of AmpC beta-lactamase, *J. Med. Chem.* 41 (1998) 4577–4586.
- [10] R.A. Powers, J. Blazquez, G.S. Weston, M.I. Morosini, F. Baquero, B.K. Shoichet, The complexed structure and antimicrobial activity of a non-beta-lactam inhibitor of AmpC beta-lactamase, *Protein Sci.* 8 (1999) 2330–2337.
- [11] S. Ness, R. Martin, A.M. Kindler, M. Paetzel, M. Gold, S.E. Jensen, J.B. Jones, N.C. Strynadka, Structure-based design guides the improved efficacy of deacylation transition state analogue inhibitors of TEM-1 beta-lactamase, *Biochemistry* 39 (2000) 5312–5321.
- [12] E. Caselli, R.A. Powers, L.C. Blaszcak, C.Y. Wu, F. Prati, B.K. Shoichet, Energetic, structural, and antimicrobial analyses of beta-lactam side chain recognition by beta-lactamases, *Chem. Biol.* 8 (2001) 17–31.
- [13] K.C. Usher, L.C. Blaszcak, G.S. Weston, B.K. Shoichet, S.J. Remington, Three-dimensional structure of AmpC beta-lactamase from *Escherichia coli* bound to a transition-state analogue: Possible impli-

- cations for the oxyanion hypothesis and for inhibitor design, *Biochemistry* 37 (1998) 16082–16092.
- [14] C. Oefner, A. D'Arcy, J.J. Daly, K. Gubernator, R.L. Charnas, I. Heinze, C. Hubschwerlen, F.K. Winkler, Refined crystal structure of beta-lactamase from *Citrobacter freundii* indicates a mechanism for beta-lactam hydrolysis, *Nature* 343 (1990) 284–288.
- [15] E. Lobkovsky, E.M. Billings, P.C. Moews, J. Rahil, R.F. Pratt, J.R. Knox, Crystallographic structure of a phosphonate derivative of the *Enterobacter cloacae* P99 cephalosporinase: mechanistic interpretation of a beta-lactamase transition-state analog, *Biochemistry* 33 (1994) 6762–6772.
- [16] A. Patera, L.C. Blaszczyk, B.K. Shoichet, Crystal structures of substrate and inhibitor complexes with AmpC beta-lactamase: Possible implications for substrate-assisted catalysis, *J. Am. Chem. Soc.* 122 (2000) 10504–10512.
- [17] W.F. Van Gunsteren, H.J.C. Berendsen, Computer-simulation of molecular-dynamics – Methodology, applications, and perspectives in chemistry, *Angew. Chem. Int. Ed. Engl.* 29 (1990) 992–1023.
- [18] L.A. Thompson, J.A. Ellman, Synthesis and applications of small molecule libraries, *Chem. Rev.* 96 (1996) 555–600.
- [19] D. Tondi, M.P. Costi, in: A. Ghose, V. Viswanadhan (Eds.), *Combinatorial Library Design and Evaluation: Principles, Software Tools and Applications in Drug Discovery*, Marcel Dekker, New York, 2001, pp. 563–603.
- [20] E.K. Kick, D.C. Roe, A.G. Skillman, G. Liu, T.J. Ewing, Y. Sun, I.D. Kuntz, J.A. Ellman, Structure-based design and combinatorial chemistry yield low nanomolar inhibitors of cathepsin D, *Chem. Biol.* 4 (1997) 297–307.
- [21] D. Tondi, U. Slomczynska, M.P. Costi, D.M. Watterson, S. Ghelli, B.K. Shoichet, Structure-based discovery and in-parallel optimization of novel competitive inhibitors of thymidylate synthase, *Chem. Biol.* 6 (1999) 319–331.
- [22] D.M. Lorber, B.K. Shoichet, Flexible ligand docking using conformational ensembles, *Protein Sci.* 7 (1998) 938–950.
- [23] D.L. Flynn, J.Z. Crich, R.V. Devraj, S.L. Hockerman, J.J. Parlow, M.S. South, S. Woodard, Chemical library purification strategies based on principles of complementary molecular reactivity and molecular recognition, *J. Am. Chem. Soc.* 119 (1997) 4874–4881.
- [24] S.G. Waley, A quick method for the determination of inhibition constants, *Biochem. J.* 205 (1982) 631–633.
- [25] E.C. Meng, B.K. Shoichet, I.D. Kuntz, Automated docking with grid-based energy evaluation, *J. Comp. Chem.* 13 (1992) 505–524.
- [26] G.V. Crichlow, A.P. Kuzin, M. Nukaga, K. Mayama, T. Sawai, J.R. Knox, Structure of the extended-spectrum class C beta-lactamase of *Enterobacter cloacae* GCl, a natural mutant with a tandem tripeptide insertion, *Biochemistry* 38 (1999) 10256–10261.
- [27] R.A. Laskowski, M.W. MacArthur, D.S. Moss, J.M. Thornton, PROCHECK: a program to check the stereochemical quality of protein structures, *J. Appl. Crystallogr.* 26 (1993) 283–291.
- [28] A. Dubus, P. Ledent, J. Lamotte-Brasseur, J.M. Frere, The roles of residues Tyr150, Glu272, and His314 in class C beta-lactamases, *Proteins* 25 (1996) 473–485.
- [29] N.C. Strynadka, H. Adachi, S.E. Jensen, K. Johns, A. Sielecki, C. Betzel, K. Sutoh, M.N. James, Molecular structure of the acyl-enzyme intermediate in beta-lactam hydrolysis at 1.7 Å resolution, *Nature* 359 (1992) 700–705.
- [30] C.C. Chen, J. Rahil, R.F. Pratt, O. Herzberg, Structure of a phosphonate-inhibited beta-lactamase. An analog of the tetrahedral transition state/intermediate of beta-lactam hydrolysis, *J. Mol. Biol.* 234 (1993) 165–178.
- [31] I.E. Crompton, B.K. Cuthbert, G. Lowe, S.G. Waley, Beta-lactamase inhibitors. The inhibition of serine beta-lactamases by specific boronic acids, *Biochem. J.* 251 (1988) 453–459.
- [32] C.L. Verlinde, W.G. Hol, Structure-based drug design: progress, results and challenges, *Structure* 2 (1994) 577–587.
- [33] P.M. Colman, Structure-based drug design, *Curr. Opin. Struct. Biol.* 4 (1994) 868–874.
- [34] D. Ringe, What makes a binding site a binding site?, *Curr. Opin. Struct. Biol.* 5 (1995) 825–829.
- [35] B.K. Shoichet, R.M. Stroud, D.V. Santi, I.D. Kuntz, K.M. Perry, Structure-based discovery of inhibitors of thymidylate synthase, *Science* 259 (1993) 1445–1450.
- [36] B.K. Shoichet, I.D. Kuntz, Predicting the structure of protein complexes: a step in the right direction, *Chem. Biol.* 3 (1996) 151–156.
- [37] N.C. Strynadka, M. Eisenstein, E. Katchalski-Katzir, B.K. Shoichet, I.D. Kuntz, R. Abagyan, M. Totrov, J. Janin, J. Cherfils, F. Zimmerman, A. Olson, B. Duncan, M. Rao, R. Jackson, M. Sternberg, M.N. James, Molecular docking programs successfully predict the binding of a beta-lactamase inhibitory protein to TEM-1 beta-lactamase, *Nature Struct. Biol.* 3 (1996) 233–239.
- [38] C.A. Kettner, R. Bone, D.A. Agard, W.W. Bachovchin, Kinetic properties of the binding of alpha-lytic protease to peptide boronic acids, *Biochemistry* 27 (1988) 7682–7688.
- [39] J. Gasteiger, M. Marsili, Electrostatic charges, *Tetrahedron* 36 (1980) 3219.
- [40] B.K. Shoichet, D.L. Bodian, I.D. Kuntz, Molecular docking using shape descriptors, *J. Comp. Chem.* 13 (1992) 380–397.
- [41] S.J. Weiner, P.A. Kollman, D.A. Case, U.C. Singh, C. Ghio, G. Alagona, J.S. Profeta, P. Weiner, A new force field for molecular mechanical simulation of nucleic acids and proteins, *J. Am. Chem. Soc.* 106 (1984) 765–784.
- [42] M.K. Gilson, B.H. Honig, Calculation of electrostatic potentials in an enzyme active site, *Nature* 330 (1987) 84–86.
- [43] Z. Otwinowski, W. Minor, Processing of X-ray diffraction data collected in oscillation mode, *Methods Enzymol.* 276 (1997) 307–326.
- [44] A.T. Brunger, P.D. Adams, G.M. Clore, W.L. DeLano, P. Gros, R.W. Grosse-Kunstleve, J.S. Jiang, J. Kuszewski, M. Nilges, N.S. Pannu, R.J. Read, L.M. Rice, T. Simonson, G.L. Warren, Crystallography and NMR system: A new software suite for macromolecular structure determination, *Acta Crystallogr. D Biol. Crystallogr.* 54 (1998) 905–921.
- [45] T.A. Jones, J.Y. Zou, S.W. Cowan, M. Kjeldgaard, Improved methods for building protein models in electron-density maps and the location of errors in these models, *Acta Crystallogr. A* 47 (1991) 110–119.
- [46] National Committee for Clinical Laboratory Standards, *Methods for Dilution Antimicrobial Susceptibility Tests for Bacteria that Grow Aerobically*. Approved Standard M7-A4, Vol. 17, National Committee for Clinical Laboratory Standards, Villanova, PA, 1997.
- [47] I.N. Topchieva, E.M. Sorokina, N.V. Efreanova, A.L. Ksenofontov, B.I. Kurganov, Noncovalent adducts of poly(ethylene glycols) with proteins, *Bioconjug. Chem.* 11 (2000) 22–29.
- [48] H.U. Bergmeyer (Ed.), *Methods of Enzymatic Analysis*, Vol. 1, Academic Press, New York, 1974.
- [49] K. Nakajima, J.C. Powers, B.M. Ashe, M. Zimmerman, Mapping the extended substrate binding site of cathepsin G and human leukocyte elastase. Studies with peptide substrates related to the alpha 1-protease inhibitor reactive site, *J. Biol. Chem.* 254 (1979) 4027–4032.
- [50] T.E. Ferrin, C.C. Huang, L.E. Jarvis, R. Langridge, The MIDAS display system, *J. Mol. Graph.* 6 (1988) 13–27.
- [51] S.V. Evans, SETOR: hardware-lighted three-dimensional solid model representations of macromolecules, *J. Mol. Graph.* 11 (1993) 134–138, 127–128.
- [52] T.J. Burnett, H.C. Peebles, J.H. Hageman, Synthesis of a fluorescent boronic acid which reversibly binds to cell walls and a diboric acid which agglutinates erythrocytes, *Biochem. Biophys. Res. Commun.* 96 (1980) 157–162.
- [53] F.R. Bean, J.R. Johnson, Derivatives of phenylboronic acid, their preparation and action upon bacteria, *J. Am. Chem. Soc.* 54 (1932) 4415–4425.